ACS Medicinal Chemistry Letters

Subscriber access provided by UNIV OF NEBRASKA - LINCOLN

Letter

Structure-guided Optimization of Replication Protein A (RPA)-DNA Interaction Inhibitors.

Navnath S. Gavande, Pamela S VanderVere-Carozza, Katherine S Pawelczak, Tyler L Vernon, Matthew Jordan, and John J. Turchi

ACS Med. Chem. Lett., **Just Accepted Manuscript** • DOI: 10.1021/acsmedchemlett.9b00440 • Publication Date (Web): 02 Jan 2020

Downloaded from pubs.acs.org on January 2, 2020

Just Accepted

"Just Accepted" manuscripts have been peer-reviewed and accepted for publication. They are posted online prior to technical editing, formatting for publication and author proofing. The American Chemical Society provides "Just Accepted" as a service to the research community to expedite the dissemination of scientific material as soon as possible after acceptance. "Just Accepted" manuscripts appear in full in PDF format accompanied by an HTML abstract. "Just Accepted" manuscripts have been fully peer reviewed, but should not be considered the official version of record. They are citable by the Digital Object Identifier (DOI®). "Just Accepted" is an optional service offered to authors. Therefore, the "Just Accepted" Web site may not include all articles that will be published in the journal. After a manuscript is technically edited and formatted, it will be removed from the "Just Accepted" Web site and published as an ASAP article. Note that technical editing may introduce minor changes to the manuscript text and/or graphics which could affect content, and all legal disclaimers and ethical guidelines that apply to the journal pertain. ACS cannot be held responsible for errors or consequences arising from the use of information contained in these "Just Accepted" manuscripts.

is published by the American Chemical Society. 1155 Sixteenth Street N.W., Washington, DC 20036

Published by American Chemical Society. Copyright © American Chemical Society. However, no copyright claim is made to original U.S. Government works, or works produced by employees of any Commonwealth realm Crown government in the course of their duties.

Structure-guided Optimization of Replication Protein A (RPA)-DNA Interaction Inhibitors.

Navnath S. Gavande,*[,†,‡] Pamela S. VanderVere-Carozza,[†] Katherine S. Pawelczak,[§] Tyler L. Vernon,[†] Matthew Jordan,[†] and John J. Turchi*[,†,§,⊥]

[†]Department of Medicine, Indiana University School of Medicine (IUSM), Indianapolis, Indiana 46202 USA

[‡]Department of Pharmaceutical Sciences, Wayne State University College of Pharmacy and Health Sciences, Detroit, Michigan 48201, USA

[§]NERx Biosciences, 212 W 10th St. Suite A480, Indianapolis, Indiana 46202, USA

[⊥]Department of Biochemistry and Molecular Biology, Indiana University School of Medicine, Indianapolis, Indiana 46202, USA

KEYWORDS: Replication Protein A, DNA damage and repair, reversible inhibitors, SAR, medicinal chemistry

ABSTRACT: Replication protein A (RPA) is the major human single stranded DNA (ssDNA)-binding protein, playing essential roles in DNA replication, repair, recombination and the DNA-damage response (DDR). Inhibition of RPA-DNA interactions represents a therapeutic strategy for cancer drug discovery and has great potential to provide single agent anticancer activity and to synergize with both common DNA damaging chemotherapeutics and newer targeted anticancer agents. In this letter, a new series of analogues based on our previously reported TDRL-551 (**4**) compound were designed to improve potency and physicochemical properties. Molecular docking studies guided molecular insights and further SAR exploration led to the identification of a series of novel compounds with low micromolar RPA inhibitory activity, increased solubility and excellent cellular up-take. Among a series of analogues, compound **43, 44, 45** and **46** hold promise for further development of novel anti-cancer agents.

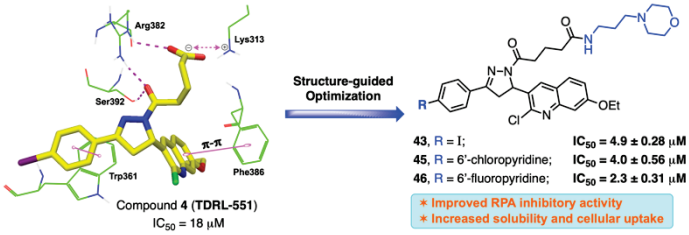

The clinical efficacy of many DNA damaging cancer chemotherapeutics involves inducing DNA damage to push cancer cells into apoptosis.[1-2] DNA damage is repaired by intrinsic repair pathways and is coordinated by the DNA damage response (DDR) pathway. One mechanism to enhance the therapeutic window associated with these therapies is to direct treatment to those cancers that harbor intrinsic DNA repair deficiencies.[3-5] This approach has been effectively exploited in synthetic lethal strategies to develop safe and effective treatments.[1] With an appropriately selected drug target, there is the potential to enhance both single agent activity and synergistic anti-cancer effect of the same chemical entity. Therefore, targeting DNA repair and the DDR deficiencies has the potential for more selective, better tolerated therapies to improve cancer patient survival.[6-7]

Replication protein A (RPA) is the major human ssDNA binding protein and plays an integral role in both nucleotide excision repair (NER) and homologous recombination (HR) DNA repair pathways in addition to its essential role in DNA replication and DDR.[8-10] Each of these critical roles of RPA make the RPA-DNA interaction a promising target to develop novel anti-cancer therapeutics. RPA is also overexpressed in a number of cancers including lung, ovarian, breast, colon and esophageal[11-12] One rationale for targeting RPA is based on RPA exhaustion which can lead to replication catastrophe. By extension, one can envision that cancer cells exhibiting replication stress require more RPA for survival compared to non-cancer cells to provide a therapeutic treatment window.

Over the past few years, several RPA inhibitors have been identified and have either focusing on blocking the protein-protein[13,15-22] or the protein-DNA interaction[14,23-26] (**Figure 1A**). Targeting the F-domain has proven effective for disrupting protein-protein interactions and the A and B domains of RPA70 for protein-DNA inhibitors.[27-29] Previously, we have successfully discovered and developed compounds **1-4** which block the RPA-DNA interaction.[23-26] Particularly, compound **3** (TDRL-505) and **4** (TDRL-551) display single agent activity in lung and ovarian cancer cell lines and also synergize with cisplatin and

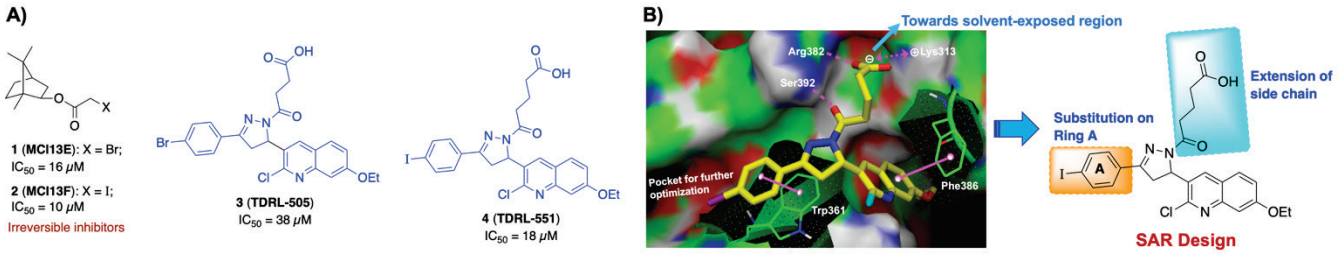

Figure 1. A) Structure of previously reported RPA inhibitors targeting RPA-DNA interaction.[23-26] **B)** Schematic representation of SAR design rationale: a large space-filling pocket surrounding Ring A of compound **4** and amino acid residues surrounding alkyl carboxylic acid side chain which can be extended towards the solvent-exposed region for further structural optimization. [Compound **4** hydrogen bond interaction with Ser392 and Arg382 is indicated with the dashed magenta line, π-π stacking interactions with Trp361 and Phe386 are shown in solid magenta dumbbell, and salt-bridge interactions with Lys313 are shown in dashed two-sided magenta arrow.]

etoposide.[25-26] The mechanism of action of both compounds is via a reversible interaction with the central OB-folds in DNA binding domains A and B of RPA70. *In vivo* analysis of compound **4** (TDRL-551) revealed minimal cytotoxicity alone and in combination with platinum was able to significantly delay tumor growth in a NSCLC xenograft model.[26] Both compounds **3** and **4,** however, had limited solubility and cell permeability. In this Letter, we further expanded our structure-guided drug design efforts by exploiting compound **4** (TDRL-551) scaffold with the aim to improve RPA inhibitory potency, solubility and cellular uptake.

Initial molecular docking studies with compounds **3** and **4** revealed that both compounds have a high predicted affinity for DNA binding domain B. We performed molecular docking studies mainly focusing on the central DNA binding domains A and B of RPA70 by using $RPA70_{181-422}$ X-ray crystal structure (PDB code: 1FGU).[29] The interaction presented in the **Figure 1B** reveals the stability is driven via hydrophobic and π-π interactions, and that the conserved alkyl carboxylic acid side chain is stabilized via interactions with basic amino acid residues which are critical for inhibitory activity. In addition, docking studies revealed the extended terminal carboxylic acid side chain appeared to orient towards the solvent-exposed region of the protein and provides a potential site for modulating the physicochemical properties of these compounds. We have exploited compound **4**'s interaction with domain B to outline a SAR design for further structural optimization (**Figure 1B**). We first pursued optimizing aromatic Ring A exploiting the large pocket around it and also simultaneously optimizing alkyl carboxylic acid side chain to improve the drug-like properties.

The synthesis of target compound **4** and its analogs **16-25** is depicted in **Scheme 1**. We have obtained compound **4** and **16-25** from starting material 3-ethoxyaniline by slightly modifying our previous synthetic protocol.[26] The requisite quinoline carbaldehyde **6** was prepared by acylation of 3-ethoxyaniline with acetic anhydride, followed by multicomponent reaction that involves process of Vilsmeier-Haack chlorination, formylation and cyclization of acetanilide using DMF and $POCl_3$. Claisen-Schmidt condensation of corresponding substituted acetophenones **7-10** with quinoline carbaldehyde **6** in the presence of aqueous NaOH in ethanol yielded corresponding 1,3-diarypropenones **11-14** which on further treatment with hydrazine hydrate in ethanol under reflux afforded the corresponding 2-pyrazolines **15a-d** in good yields. Compound **4** and **16-18** were obtained in good yields by acylation at N1 of the pyrazoline ring of compounds **15a-d** with glutaric anhydride in chloroform. Upon reduction of nitro group of **18** by stannous chloride, the desired amine product **19** was obtained in an acceptable yield. The synthesis of compound **20** and **21** was accomplished by acylation of hydroxyl group of compound **17** using acryloyl chloride and morpholinecarbonyl chloride, respectively, in basic condition. To further extend the substitution on *para*-position at ring A, we have synthesized target compounds **22-29** as depicted in **Scheme 1** and supplemental **Scheme S1**. Compound **30** was prepared from an above synthesized precursor **15a** by N1-acylation of the pyrazoline ring using ethyl glutaryl chloride in basic condition. Intermediates **31a-d** were prepared by optimizing Pd-catalyzed Suzuki coupling of compound **30** with corresponding boronic acids/esters using non-aqueous CsF in dimethoxyethane protocol. Final target compounds **22-25** were obtained from compounds **31a-d** by hydrolysis of corresponding alkyl esters using 10N NaOH at room temperature. Our initial attempt utilizing **Scheme 1** to synthesize halopyridine containing compounds **26-28** had limited efficiency as a function of the late stage Suzuki coupling reaction. Therefore, we have achieved efficient synthesis of target compounds **26-29** as outlined in Supplemental **Scheme S1**. Early stage Suzuki coupling of 4′-iodoacetophenone **7** with commercially available boronic acids/esters **32a-d** catalyzed by tetrakis(triphenylphosphine)palladium(0) in the presence of aqueous potassium carbonate base provided precursors **33a-d**. 1,3-diarypropenones **34a-d** were synthesized using an above described Claisen-Schmidt condensation of corresponding substituted methyl ketones **33a-d** with quinoline carbaldehyde **6** then 1,3-diarypropenones **34a-d** refluxed with hydrazine hydrate in ethanol to afford corresponding 2-pyrazolines **35a-d** in good yields. Finally, acylation at N1 of the pyrazoline ring of compounds **35a-d** with glutaric anhydride in chloroform under reflux provided target compounds **26-29** in moderate to good yields after recrystallization in ethanol.

To optimize the alkyl carboxylic acid side chain of compound **4,** we have synthesized compounds **37-47** as depicted in Supplemental **Schemes S2 and S3**. The N1-acylation of the pyrazoline ring of precursor **15a** using alkyl acyl chloride in basic conditions afforded ester derivatives **36a-b** and subsequent ester hydrolysis using NaOH, provided analogs **37-38** in excellent yields (Supplemental **Scheme S2**). To introduce rigidity in the RPA binding pocket, we have synthesized compounds **39-40**

Scheme 1. Synthesis of Compound 4 and Analogs 16-25[a]

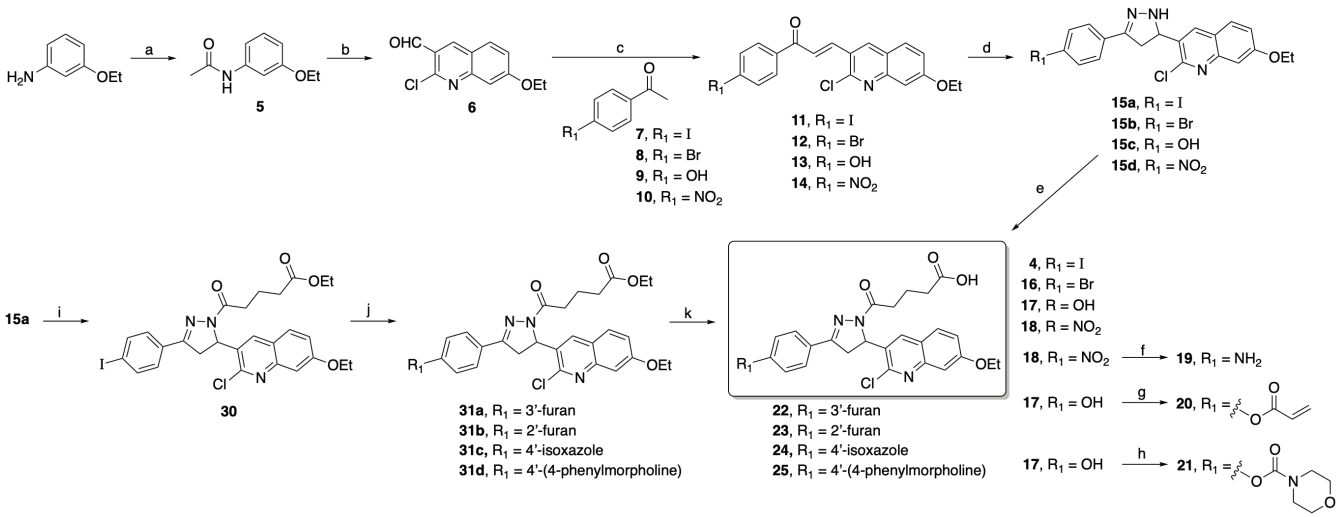

[a]Reagents and conditions: (a) acetic anhydride, DIPEA, DMAP, DCM, rt for 2 h, 88%; (b) (i) DMF, $POCl_3$, 0°C for 25 min, (ii) acetanilide **5**, 110°C for 3 h, 74%; (c) 2.5M NaOH, EtOH, 45°C for 45 min to 1 hr, 53-74%; (d) hydrazine hydrate, EtOH, reflux for 2-3 h, 70-83%; (e) glutaric anhydride, $CHCl_3$, reflux for 2 h, 58-71% (after recrystallization); (f) $SnCl_2$, EtOH:THF (1:1), reflux for 2 h, 48% (after recrystallization); (g) acryloyl chloride, 2N NaOH, THF, 0°C to rt for 2 h, 34%; (h) 4-morpholinecarbonyl chloride, TEA, DMAP, THF, 0°C to rt for 12 h, 63%. (i) ethyl glutaryl chloride, DIPEA, DCM, rt for 12 h, 78%; (j) boronic acid/ester, $Pd(PPh_3)_4$, CsF, DME, 90°C for 15-18 h, 63-69%; (k) 10N NaOH, THF:MeOH (1:2), rt for 6-8 h, 75-87%.

from precursor **11** and using corresponding substituted hydrazinobenzoic acid under reflux condition in AcOH and *n*-butanol. Furthermore, the morpholine/morpholinoalkylamine group was attached to the oxopentanoic acid side chain of corresponding compound **4** or **16** or **26** or **28** or **29** by utilizing EDCI/HOBt amide synthetic protocol to achieve final compounds **41-47** in good yields (Supplemental **Scheme S3**).

The assessment of RPA inhibitory activity was performed using a highly sensitive and quantitative electrophoretic mobility shift assay (EMSA). The assay employs purified heterotrimeric human RPA devoid of any tags or modifications and measures the impact of the compounds on direct RPA binding to a ss-DNA substrate.[23,26,30] We also have confirmed that the compounds specifically target OB-folds A and B using an RPA construct consisting of this minimal DNA binding domain (See **Supplemental Table S2**), as we have previously described.[25] RPA can also interact with damage duplex DNA via binding to the undamaged ssDNA regions opposite the damage.[30] The RPA inhibitory compounds also, as expected, block this interaction. For the purpose of quantifying RPA inhibitory activity we used gold-standard, full length RPA binding to single stranded DNA to calculated IC_{50} values of newly synthesized analogs and provide insight into the structure-activity relationships (**Table 1** and **2**). The replacement of the iodo group of compound **4** (IC_{50} = 15.3 ± 1.42 μM) with hydroxyl or nitro groups resulted in a near complete loss of RPA inhibitory activity while changing to an amine resulted in a 7-fold increase in potency (IC_{50} = 2.3 ± 0.22 μM). Acrylate containing compound **20** exhibited 2-fold increase in activity compared to **4**, surprisingly, the inclusion of morpholinecarbonyl group in compound **21** resulted in poor RPA inhibition. Introduction of a heteroaromatic on Ring A such as 3'-furan, 2'-furan and 4'-isoxazole boosted potency drastically as 2'-substituted furan at Ring A (compound **23,** IC_{50} = 2.1 ± 0.48 μM) exhibited almost 3.2-fold increase in activity compared to 3'-substituted furan containing compound **22** (IC_{50} = 6.7 ± 0.64 μM). Insertion of another heteroatom such as nitrogen into the furan ring in the form of an isoxazole displayed even more potent RPA inhibitory activity (compound **24**, IC_{50} = 1.7 ± 0.28 μM). The difference in activity with the small changes of heteroatom within 5-membered ring may be due to the orientation of the ring or ability of the heteroatom to interact with RPA backbone binding pocket amino acid residues. Further extension of compound **4** Ring A in the space-filling binding cleft with a substituted bulky biphenyl heteroaromatic ring such as halogenated pyridinyl compounds (**26-29**) exhibited even more potent RPA inhibitory activities than parent compound with an increased potency between 4- and 15-fold. Among all the Ring A modifications, chloro-pyridinyl compound **26** and bromo-pyridinyl compound **27** showed the most potent RPA inhibitory activity in the EMSA assay (**26**, 1.6 ± 0.04 μM and **27**, IC_{50} = 1.0 ± 0.60 μM). Further, we have included fluorine and trifluoromethyl substituents in pyridinyl compounds **28-29**. However, both compounds displayed slightly weaker activity compared to chloro- and bromo-pyridinyl containing compounds **26-27.** These data revealed the importance of bulky hydrophobic substituents on Ring A of compound **4** to occupy space-filling binding pocket of RPA and are consistent with our postulated molecular docking binding pockets outlined in an above SAR design section.

The next aim was to explore SAR on the alkyl carboxylic acid side chain of compound **4**, with a focus on enhancing physicochemical properties while retaining or improving potency. Modification of alkyl side chain of compound **4** revealed a series of interesting activity against RPA (**Supplemental Table S1**). The conversion to an oxopentanoic ethyl ester (compound **30**) completely abrogated RPA inhibitory activity. A similar trend was observed with compounds **39-40** when we replaced oxopentanoic acids with 2' or 3'-subsitituted benzoylic carboxylic acids. The intramolecular distances between the benzoylic carboxylic acids and the core dihydropyrazole

Table 1. SAR of Ring A with RPA IC_{50} Values of Analogs 16-29[a]

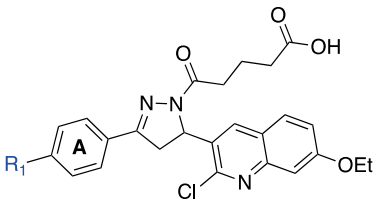

Cpd	R_1	RPA IC_{50} (μM)[b,c]
4	I	15.3 ± 1.42
16	Br	19.2 ± 4.17
17	OH	>25
18	NO_2	>25
19	NH_2	2.3 ± 0.22
20		8.9 ± 0.98
21	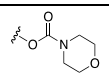	>25
22		6.7 ± 0.64
23		2.1 ± 0.48
24		1.7 ± 0.28
25	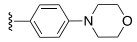	3.1 ± 0.23
26	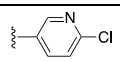	1.6 ± 0.04
27	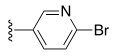	1.0 ± 0.60
28	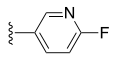	2.6 ± 0.60
29	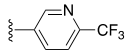	4.3 ± 0.42

[a]Determined using EMSA, binding of full length human RPA to DNA was assessed. [b]Compounds that displayed greater than 80% inhibition at 25 μM were analyzed in titration experiments. [c]IC_{50} values are a mean of minimum of triplicate independent experiments and data are presented as the mean ± SD.

were very similar comparing to the oxopentanoic acids. The dramatic reduction in activity of the benzoylic carboxylic acid derivatives is likely function on the rigidity induced restricting motion of the molecule within the RPA-DNA binding pocket independent of position of the carboxylic acid. Increasing the length of the aliphatic side chain by 1 and 2 carbon, in compounds **37** and **38** respectively, had only modest effects on potency and similar inhibition was observed by direct addition of a *N*-morpholino group on alkyl carboxylic acid side chain depicted in compound **41**

As discussed earlier, initial docking study positioned the terminal carboxylic group towards the solvent-exposed region of the protein and could provide a good potential for modulating the physicochemical properties of our compounds. In addition, carboxylic acid functional group often have limited utility in drug discovery due to limited passive diffusion across biological membranes (cellular permeability) and metabolic instability.[31] Therefore, we articulated that RPA inhibitors could be improved by introducing an additional solubilizing group into the terminal carboxylic acid group without significantly influencing the RPA inhibitory activities. To this end, the water-soluble morpholine moiety was employed to enhance the physicochemical properties. Consistent with our docking analysis, replacement of the terminal carboxylic group with morpholinoethane (compound **42**) and morpholinopropane (compound **43**), retained the inhibitory activity while compound **43** showed an almost 3-fold increase in potency (IC_{50} = 4.9 ± 0.28 μM) compared to our parent compound **4**. Encouraged by these results, a series of new analogs (**Table 2**, compounds **44-47**) were further designed and synthesized by incorporating morpholinopropane at the terminal carboxylic group of compound **16, 26 and 28-29**. All these compounds exhibited modest to potent RPA inhibitory activity compared to the parent compound **4** and anticipated to improve physiochemical properties for better cellular and *in vivo* activities.

Table 2. SAR of Side Chain Modifications with RPA IC_{50} Values of Analogs 41-47[a]

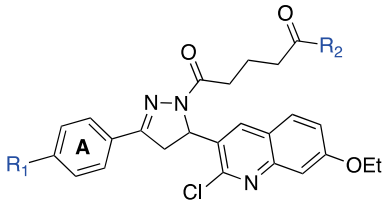

Cpd	R_1	R_2	RPA IC_{50} (μM)[b,c]
41	I		6.6 ± 0.48
42	I	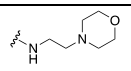	10.5 ± 0.68
43	I	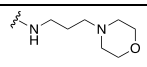	4.9 ± 0.28
44	Br	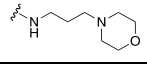	10.0 ± 1.46
45	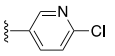	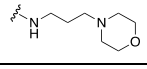	4.0 ± 0.56
46	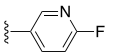	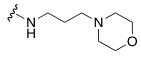	2.3 ± 0.31
47	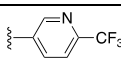	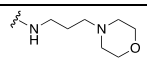	5.8 ± 0.39

[a]Determined using EMSA, binding of full length human RPA to DNA was assessed. [b]Compounds that displayed greater than 80% inhibition at 25 μM were analyzed in titration experiments. [c]IC_{50} values are a mean of minimum of triplicate independent experiments and data are presented as the mean ± SD.

To confirm the mechanism of inhibitions *via* compound binding to the target protein and not *via* binding to the DNA substrates, we conducted a fluorescent intercalator displacement (FID) assay as described previously.[32] The displacement of a DNA binding dye and decrease in fluorescence is indicative of the compound's

ability to bind DNA. In order to probe the potential role of DNA intercalation as a mechanism for RPA inhibition, most potent compounds **19, 23, 26, 27, 43** and **45** were analyzed using FID assay along with doxorubicin (Dox) as a positive control. The results presented in **Figure 2** demonstrate as expected that positive control, doxorubicin a known non-covalent DNA binding chemotherapeutic, resulted in a concentration dependent reduction in fluorescence. As expected, minimal DNA binding activity was observed for any of the novel RPA inhibitors (**19, 23, 26, 27, 43** and **45**). The slight reduction in signal cannot account for the

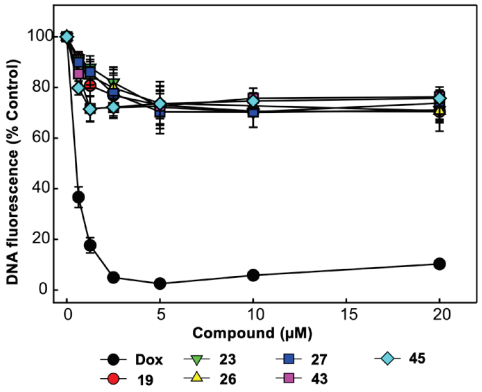

Figure 2. Analysis of compound interactions with DNA using Fluorescent intercalator displacement (FID) assay. The indicated concentrations of doxorubicin (Dox), compounds **19**, **23**, **26**, **27**, **43** and **45** were analyzed for the ability to displace a fluorescent Sybr-green DNA intercalator as a measure of compound DNA interactions. The data represent the average and SD of three independent experimental determinations performed in duplicates.

high potency of the compounds. These data suggest that the mechanism of action involves targeting the protein- DNA interaction by directly binding to the RPA protein. Consistent with this conclusion is the lack of inhibitory agains other OB-fold containing proteins

To delineate the key interactions and to understand the SAR of newly synthesized compounds, these compounds were flexibly docked mainly focusing on the central DNA binding domains A and B of RPA70 as discussed above.[29] All newly developed inhibitors docked well at this site. **Figure 3** shows the binding orientation and molecular interactions of representative compound **26, 42** and **45** within the RPA domain B region. The molecular interaction of **26**, **42** and **45** (**Figures 3A-C, respectively**) is largely ascribed to various electrostatic interactions, including, i) compound **42** and **45** amide carbonyl make hydrogen bond contacts with the amine of Lys313, while compound **26** terminal carboxylic acid makes salt-bridge interactions with the Lys313; ii) amide carbonyl (attached to pyrazole ring) of all three compounds make strong hydrogen bond contacts with the hydroxyl group of Ser392 as well as with the amine group of Arg382; iii) the π – π stacking interactions between the phenyl moiety (Ring A) and the aromatic ring of Trp361 in all three compounds. In addition, all three compounds quinoline moiety is also well positioned to make π – π stacking interactions with Phe386; iv) Terminal alkyl morpholino side chain is well fitted and located as its extending out of the RPA binding region into a solvent exposed region. Docking studies predicted a stronger affinity of the compound **26** than other series of compounds including compound **42** and **45,** in fact compound **26** also showed potent RPA inhibition than other series of compounds in *in-vitro* EMSA assay **(Table 1)**.

Our previous data demonstrated that compound **3** and **4** displayed a significantly higher cellular IC_{50} compared to the biochemical *in vitro* IC_{50}.[25-26] This suggested cellular uptake could be limiting cellular activity. The charge on the carboxylic acid, while potentially increasing aqueous solubility, was also anticipated to negatively impact cellular uptake. We therefore assessed aqueous solubility of a series of the most biochemically active compound **4** derivatives. **Figure 4A** shows data obtained with assessing aqueous solubility in unbuffered H_2O at pH 7. The data reveal a general trend of the morpholino modified compounds displaying increased solubility compared to their carboxylic acid counterparts (compounds **4, 16, 26, 28, 29** *Vs* **43, 44, 45, 46, 47**, respectively).

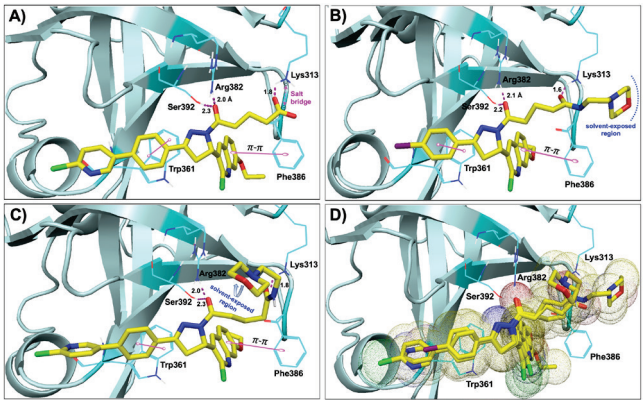

Figure 3. Molecular docking studies (PDB code: 1FGU)[29]: **A-C)** Molecular interactions of compound **26** (**A**), **42** (**B**) and **45** (**C**) (all in yellow carbon) with hRPA (key amino acids are shown in dark cyan carbon and cartoon is shown in pale cyan color). Interaction with amino acid side chains is indicated with the dashed magenta lines, π – π stacking interactions are shown in solid magenta dumb ell and salt-bridge interactions are shown in dashed two-sided magenta arrow. Interaction distances indicated in Å. **D)** Molecular overlay (superimposition) of compound **26, 42** and **45** (all in yellow carbon) in the RPA binding site.

The cellular uptake or intracellular metabolism of the compounds plays an important role in cellular efficacy and it allows to properly rationalize structure-activity relationships to enhance the sustained therapeutic effect. Therefore, we evaluated cellular uptake of our lead compounds in H460 NSCLC cells (**Figure 4B**). The data demonstrate that as expected that compound **4** has relatively poor uptake while compound **26** showed increased uptake even with the carboxylic acid moiety. The morpholino derivative of these both compounds demonstrated considerably superior uptake observed with the compounds **43** and **45.** We expect the increased uptake will increase cellular RPA inhibition and anti-cancer activity. A similar trend of increased cellular uptake was also observed in morpholino modified compound **46** and **47** compared to their carboxylic acid counterparts (Data not shown).

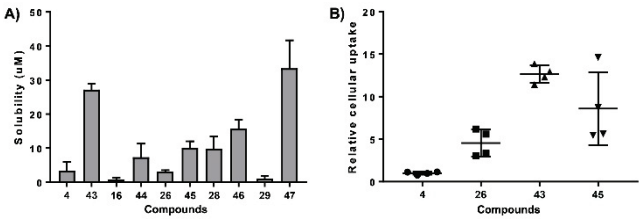

Figure 4. Solubility analysis and cellular uptake of RPA inhibitors. **A**) Aqueous solubility and **B**) Cellular uptake of representative compounds were determined as described in the "Supporting

Information". Individual data points are plotted and bars represent the mean and SD of three independent experimental determinations.

In conclusion, we have extended SAR study of our previously reported RPA inhibitor by utilizing a structure-based drug design strategy. We have identified a series of novel chemical inhibitors that interact directly with RPA to block its interaction with single-stranded DNA and most importantly these inhibitors do not bind directly with DNA. The systematic SAR exploration had revealed that a heteroaromatic ring or reasonably a larger lipophilic biphenyl ring at the Ring A and an extension of the terminal carboxylic acid side chain are well tolerated. Particularly, the introduction of morpholino group at the terminal alkyl carboxylic acid side chain resulted in the enhanced potency, solubility and cellular up-take. Compound **43**, **45** and **46** represent excellent lead compounds with drug-like properties suitable for future cellular and *in vivo* studies. These efforts will be addressed in a subsequent manuscript.

ASSOCIATED CONTENT

Supporting Information

Supplementary Figures S1, synthetic Schemes S1-S3, Table S1, and Table S2, synthetic experimental procedures along with characterization data, biological and physiochemical experimental procedures, copies of ^{1}H NMR spectra of final compounds, molecular docking overlays and 2D interactions of RPA inhibitors with RPA protein.

The Supporting Information is available free of charge on the ACS Publications website.

Conflict of Interest Disclosure

J Turchi is a co-founder of NERx Biosciences and receives research funding from NERx Biosciences.

AUTHOR INFORMATION

Corresponding Authors

*John J. Turchi: E-mail Address: jturchi@iu.edu (JJT). Tel.: +1-(317)-278-1996; fax, +1-(317)-274-0396.

*Navnath S. Gavande: E-mail Address: ngavande@wayne.edu (NSG). Tel.: +1-(313)-577-1523; fax, +1-(313)-577-2033.

ORCID

Navnath S. Gavande: 0000-0002-2413-0235
John J. Turchi: 0000-0001-5375-2992

Author Contributions

The manuscript was written by N.S.G. and J.J.T. with editing support from P.S.V., K.S.P., M.J., and T.L.V. All authors have given approval to the final version of the manuscript.

Funding Sources

This work is supported by NIH grants R01-CA180710 and R41-CA162648 and the Tom and Julie Wood Family Foundation.

ACKNOWLEDGMENT

We thank Dr. Lifan Zeng and Erica Woodall for technical assistance with HPLC and mass spectrometry (LCMS and HRMS).

ABBREVIATIONS

DDR, DNA Damage Response; NER, Nucleotide Excision Repair; RPA, Replication Protein A; DBD, DNA Binding Domain; HOBt, Hydroxybenzotriazole; EDCI, 1-Ethyl-3-(3-(dimethylamino)propyl)-carbodiimide; DIPEA, *N,N*-Diisopropylethylamine; DMAP, 4-Dimethylaminopyridine; DCM, Dichloromethane; DMF, N,N-Dimethylformamide; THF, Tetrahydrofuran; TEA, Triethylamine; DME, Dimethoxyethane; EMSA, Electrophoretic Mobility Shift Assay; SAR, Structure Activity Relationship; FID, Fluorescent Intercalator Displacement; Dox, Doxorubicin

REFERENCES

(1) Gavande, N. S.; VanderVere-Carozza, P. S.; Hinshaw, H. D.; Jalal, S. I.; Sears, C. R.; Pawelczak, K. S.; Turchi, J. J. DNA repair targeted therapy: The past or future of cancer treatment? *Pharmacol. Ther.* **2016**, *160*, 65-83.

(2) Willers, H.; Azzoli, C. G.; Santivasi, W. L.; Xia, F. Basic mechanisms of therapeutic resistance to radiation and chemotherapy in lung cancer. *Cancer J.* **2013**, *19*, 200-207.

(3) Blackford, A. N.; Jackson, S. P. ATM, ATR, and DNA-PK: The trinity at the heart of the DNA Damage Response. *Mol. Cell.* **2017**, *66*, 801-817.

(4) Brown, J. S.; O'Carrigan, B.; Jackson, S. P.; Yap, T. A. Targeting DNA repair in cancer: Beyond PARP inhibitors. *Cancer Discov.* **2017**, *7*, 20-37.

(5) Jackson, S. P.; Helleday, T. Drugging DNA repair. *Science* **2016**, *352*, 1178-1179.

(6) Hosoya, N.; Miyagawa, K. Targeting DNA damage response in cancer therapy. *Cancer Sci.* **2014**, *105*, 370-388.

(7) O'Connor, M. J. Targeting the DNA Damage Response in Cancer. *Mol. Cell.* **2015**, *60*, 547-560.

(8) Oakley, G. G.; Patrick, S. M. Replication Protein A: directing traffic at the intersection of replication and repair. *Front Biosci.* **2010**, *15*, 883-900.

(9) Binz, S. K.; Sheehan, A. M.; Wold, M. S. Replication Protein A phosphorylation and the cellular response to DNA damage. *DNA Repair* **2004**, *3*, 1015-1024.

(10) Marechal, A.; Zou, L. RPA-coated single-stranded DNA as a platform for post-translational modifications in the DNA damage response. *Cell. Res.* **2015**, *25*, 9-23.

(11) Planchard, D.; Domont, J.; Taranchon, E,; Monnet, I.; Tredaniel, J.; Caliandro, R.; Validire, P.; Besse, B.; Soria, J.-C.; Fouret, P. The NER proteins are differentially expressed in ever smokers and in never smokers with lung adenocarcinoma. *Ann. Oncol.* **2009**, *20*, 1257-1263.

(12) Jekimovs, C.; Bolderson, E.; Suraweera, A.; Adams, M.; O'Byrne, K. J.; Richard, D. J. Chemotherapeutic compounds targeting the DNA double-strand break repair pathways: the good, the bad, and the promising. *Front. Oncol.* **2014**, *4*, 86.

(13) Patrone, J. D.; Waterson, A. G.; Fesik, S. W. Recent advancements in the discovery of protein–protein interaction inhibitors of replication protein A. *MedChemComm* **2017**, *8*, 259-267.

(14) Gavande, N. S.; VanderVere-Carozza, P. S.; Pawelczak, K. S.; Turchi, J. J. Targeting the nucleotide excision repair pathway for therapeutic applications. In DNA Repair in Cancer Therapy: Molecular Targets and Clinical Applications; Kelley, M., Ed.; Elsevier Academic Press: Amsterdam, The Netherlands, 2016; pp 135-150.

(15) Patrone, J. D.; Kennedy, J. P.; Frank, A. O.; Feldkamp, M. D.; Vangamudi, B.; Pelz, N. F.; Rossanese, O. W.; Waterson, A. G.; Chazin, W. J.; Fesik, S. W. Discovery of protein-protein interaction inhibitors of replication protein A. *ACS Med. Chem. Lett.* **2013**, *4*, 601-605.

(16) Feldkamp, M. D.; Frank, A. O.; Kennedy, J. P.; Patrone, J. D.; Vangamudi, B.; Waterson, A. G.; Fesik, S. W.; Chazin, W. J. Surface reengineering enables co-crystallization with an inhibitor of the RPA interaction motif of ATRIP. *Biochemistry* **2013**, *52*, 6515-6524.

(17) Glanzer, J. G.; Carnes, K. A.; Soto, P.; Liu, S.; Parkhurst, L. J.; Oakley, G. G. A Small Molecule Directly Inhibits the p53 Transactivation Domain from Binding to Replication Protein A. *Nucleic Acids Res*., **2013**, *41*, 2047-2059.
(18) Frank, A.O; Feldkamp, M.D.; Kennedy, J. P.; Waterson, A. G. Pelz, N. F.; Patrone, J. D.; Vangamudi, B.; Camper, D. V.; Rossanese, O. W.; Chazin, W. J.; Fesik, S. W. Discovery of a Potent Inhibitor of Replication Protein A Protein−Protein Interactions Using a Fragment-Linking Approach. *J. Med. Chem.*, **2013**, *56*, 9242-9250.
(19) Frank, A. O.; Vangamudi, B.; Feldkamp, M. D.; Souza-Fagundes, E. M.; Luzwick, J. W.; Cortez, D.; Olejniczak, E. T.; Waterson, A. G.; Rossanese, O. W.; Chazin, W. J.; Fesik, S. W. Discovery of a potent stapled helix peptide that binds to the 70N domain of replication protein A. *J. Med. Chem.* **2014**, *57*, 2455−2461.
(20) Glanzer, J. G.; Liu, S.; Wang, L.; Mosel, A.; Peng, A.; Oakley, G. G. RPA Inhibition Increases Replication Stress and Suppresses Tumor Growth. *Cancer Res.*, **2014**, *74*, 5165-5172.
(21) Waterson, A. G.; Kennedy, J. P.; Patrone, J. D.; Pelz, N. F.; Feldkamp, M. D.; Frank, A. O.; Vangamudi, B.; Souza-Fagundes, E. M.; Rossanese, O. W.; Chazin, W. J.; Fesik, S. W. Diphenylpyrazoles as replication protein a inhibitors. *ACS Med. Chem. Lett*. **2015**, *6*, 140-145.
(22) Patrone, J. D.; Pelz, N. F.; Bates, B. S.; Souza-Fagundes, E. M.; Vangamudi, B.; Camper, D. V.; Kuznetsov, A. G.; Browning, C. F.; Feldkamp, M. D. Frank, A. O.; Gilston, B. A.; Olejniczak, E. T.; Rossanese, O. W.; Waterson, A. G.; Chazin, W. J.; Fesik, S. W. Identification and optimization of anthranilic acid-based Inhibitors of replication protein A. *ChemMedChem* **2016**, *11*, 893-899.
(23) Andrews, B. J.; Turchi, J. J. Development of a high-throughput screen for inhibitors of replication protein A and its role in nucleotide excision repair. *Mol. Cancer Ther*. **2004**, *3*, 385-391.
(24) Neher, T. M.; Bodenmiller, D.; Fitch, R. W.; Jalal, S. I.; Turchi, J. J. Novel irreversible small molecule inhibitors of replication protein A display single-agent activity and synergize with cisplatin. *Mol. Cancer Ther*. **2011**, *10*, 1796-1806.
(25) Shuck, S. C.; Turchi, J. J. Targeted inhibition of replication protein A reveals cytotoxic activity, synergy with chemotherapeutic DNA-damaging agents, and insight into cellular function. *Cancer Res*. **2010**, *70*, 3189-3198.
(26) Mishra, A. K.; Dormi, S. S.; Turchi, A. M.; Woods, D. S.; Turchi, J. J. Chemical inhibitor targeting the replication protein A–DNA interaction increases the efficacy of Pt-based chemotherapy in lung and ovarian cancer. *Biochem. Pharmacol*. **2015**, *93*, 25-33.
(27) Brosey, C. A.; Soss, S. E.; Brooks, S.; Yan, C.; Ivanov, I.; Dorai, K.; Chazin, W. J. Functional dynamics in replication protein a DNA binding and protein recruitment domains. *Structure* **2015**, *23*, 1028-1038.
(28) Fan, J.; Pavletich, N. P. Structure and conformational change of a replication protein A heterotrimer bound to ssDNA. *Genes Dev.* **2012**, *26*, 2337-2347.
(29) Bochkareva, E.; Belegu, V.; Korolev, S.; Bochkarev, A. Structure of the major single-stranded DNA-binding domain of replication protein A suggests a dynamic mechanism for DNA binding. *EMBO J.* **2001**, *20*, 612-618.
(30) Patrick, S. M.; Turchi, J. J.; Replication protein A (RPA) binding to duplex cisplatin damaged DNA is mediated through the generation of single-stranded DNA. *J. Biol. Chem.* **1999**, *274*, 14972-14978.
(31) Lassalas, P.; Gay, B.; Lasfargeas, C.; James, M. J.; Tran, V.; Vijayendran, K. G.; Brunden, K. R.; Kozlowski, M. C.; Thomas, C. J.; Smith, AB III; Huryn, D. M.; Ballatore, C. Structure Property Relationships of Carboxylic Acid Isosteres. *J. Med. Chem.* **2016**, *59*, 3183-3203.
(32) Gavande, N. S.; VanderVere-Carozza, P. Mishra, A. K.; Vernon, T. L.; Pawelczak, K. S.; Turchi, J. J. Design and Structure-Guided Development of Novel Inhibitors of the Xeroderma Pigmentosum Group A (XPA) Protein-DNA Interaction. *J. Med. Chem.* **2017**, *60*, 8055-8070.

Table of Contents Graphic: